Mg^{2+} and magnesium ammonium phosphate (MAP)-induced anammox granulation for comparable nitrogen removal

Implementation pathways and microbial mechanisms

Shi, Huiqun; Ren, Xiaoyi; Yang, Ruili; Wang, Jinsong; Xu, Huaihao; Liao, Xinqing; Lou, Yaoyin; Chen, Shaohua; Ye, Xin; Wang, Xiaojun

DOI
10.1016/j.watres.2024.122954

Publication date
2025

Document Version
Final published version

Published in
Water Research

Water Research 272 (2025) 122954

Contents lists available at ScienceDirect

Water Research

journal homepage: www.elsevier.com/locate/watres

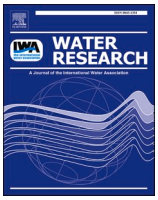

Mg^{2+} and magnesium ammonium phosphate (MAP)-induced anammox granulation for comparable nitrogen removal: Implementation pathways and microbial mechanisms

Huiqun Shi [a,b,1], Xiaoyi Ren [a,c,1], Ruili Yang [d], Jinsong Wang [e], Huaihao Xu [a,c], Xinqing Liao [a,c], Yaoyin Lou [a], Shaohua Chen [a], Xin Ye [a,*], Xiaojun Wang [a,*]

[a] CAS Key Laboratory of Urban Pollutant Conversion, Institute of Urban Environment, Chinese Academy of Sciences, Xiamen 361021, China
[b] College of Resources and Environment, Fujian Agriculture and Forestry University, Fuzhou 350002, China
[c] University of Chinese Academy of Sciences, Beijing 100049, China
[d] Yancheng Institute of Technology, Jiangsu, Yancheng 224051, China
[e] Department of Biotechnology, Delft University of Technology, Van der Maasweg 9, 2629 HZ, Delft, the Netherlands

ARTICLE INFO

Keywords:
Anammox granulation
Ion adsorption
Map precipitation
Flotation control
Metatranscriptomics and metabolomics

ABSTRACT

Anaerobic ammonium oxidation (anammox) process is a highly effective and economic technology for nitrogen removal from wastewater. However, the slow growth of anammox bacteria and sludge flotation often hinder its field application. Ion adsorption and crystal precipitation can potentially promote the sludge granulation and hence address the above issues. This study investigated two approaches to support anammox granulation through Mg^{2+} adsorption and magnesium ammonium phosphate (MAP) precipitation. Mg^{2+} addition improved the specific anammox activity (SAA) by 4.09 to 4.75-fold compared to MAP-mediated ones, which could be explained by the upregulations of nitrogen and inorganic carbon metabolisms. The active extracellular polymeric substances generation at metabolites level may also favor the granulation in Mg^{2+}-mediated anammox. However, sludge loss halted the continuous size increase of sludge. Differently, MAP promoted granulation by physically increasing the granular density, which allowed for a greater retention of sludge within the reactor. However, the co-growth of MAP precipitates with anammox may lead to mass transfer limitations, resulting in down-regulated gene expressions and metabolites in inorganic carbon metabolism, which negatively impacted the SAA. Overall, both strategies achieved comparable nitrogen removal capacities. Nevertheless, the co-growth of MAP and anammox was promising for effectively mitigating sludge flotation. Our study provided strategies and omics-based evidences for anammox granulation and activity variations, benefiting anammox practical applications.

1. Introduction

Anaerobic ammonium oxidation (anammox), as a promising autotrophic nitrogen removal process, receives much concerns in both fundamental and applied research due to high nitrogen removal efficiency, low energy consumption, and no organic carbon needed (Kartal et al., 2010). However, in a well-established annamox system, when anammox bacteria successfully aggregate, a large number of produced N_2-bubbles cannot be exhausted in time and are trapped in sludge. This may cause sludge flotation and washout, thereby leading to an instability or even complete deterioration of the biological system. Some studies addressed this issue by agitating, enhancing shear force, or crushing floating granular anammox and returning the suspension to the system (Chen et al., 2010; Lu et al., 2012; Song et al., 2017). Nevertheless, the implementation of these artificial measures requires additional energy input and meticulous control over system operations.

Granulation is proposed as an alternative to improve the sedimentation property of sludge, maintain the anammox biomass, and overcome the adverse external environment (Pol et al., 2004; Zhang et al., 2016). Microbial aggregation often occurs under high hydraulic

* Corresponding authors at: CAS Key Laboratory of Urban Pollutant Conversion, Institute of Urban Environment, Chinese Academy of Sciences, 1799 Jimei Road, Xiamen 361021, China.
E-mail addresses: 903318781@qq.com (H. Shi), xiaoyiren@iue.ac.cn (X. Ren), rlyang1989@163.com (R. Yang), J.Wang-18@tudelft.nl (J. Wang), hhxu@iue.ac.cn (H. Xu), xqliao@iue.ac.cn (X. Liao), yylou@iue.ac.cn (Y. Lou), shchen@iue.ac.cn (S. Chen), xye@iue.ac.cn (X. Ye), xjwang@iue.ac.cn (X. Wang).
[1] means the authors contribute equally.

https://doi.org/10.1016/j.watres.2024.122954
Received 3 July 2024; Received in revised form 26 September 2024; Accepted 9 December 2024
Available online 10 December 2024

selection pressure, where the change increases hydrophobicity of cell surface, triggers cell-to-cell adhesion and hence a microbial self-aggregation (Liu et al., 2004). Furthermore, the addition of divalent cations, such as Ca^{2+}, Fe^{2+}, Mg^{2+}, can serve as important promoters for granulation by reducing electrostatic repulsion through compressing the double layer and shortening the distance between individual bacterial cells, thereby facilitating particle formation (Fu et al., 2017; Jiang et al., 2003; Wu et al., 2015). Conversely, another study reported that Mg^{2+} may be detrimental granulation as it can promote the degradation of second messenger cyclic diguanylate (Zhen et al., 2021). This presents a contradiction regarding the role of divalent cations in granulation. Moreover, the use of divalent cation-based crystal precipitation has been proposed to promote granulation, with additional benefit of simultaneous phosphorus recovery (Lin et al., 2019; Li et al., 2024). For example, hydroxyapatite (HAP) was formed in anammox granules with the excellent settleability (Lin et al., 2019). The advantages of HAP-anammox sludge system was also verified in a low-strength ammonium wastewater treatment plant (Guo et al., 2021). Recently, Li et al. (2024) also achieved the synchronous growth of anammox-magnesim ammonium phosphate (MAP) granules through harnessing the cooperative action of microorganisms. Both ion adsorption and crystal precipitation have demonstrated effective nitrogen removal; however, a systematic comparison of the anammox granulation processes mediated by ion adsorption and crystal precipitation is warranted, which not only evaluates their impacts on sludge characteristics as previous studies have done, but also delves deeper into the bacterial response mechanisms.

Metabolisms for nitrogen, carbon, purine, pyrimidine, extracellular polymeric substances, signaling molecular, etc. are essential to anammox physiology, since they significantly affected the processes of energy generation, bacterial growth, aggregation, and communication (Kouba et al., 2022; Ma et al., 2020). Anammox phenotype was regulated by a complex network. Metatranscriptomics and metabolomics are able to characterized cellular metabolic pathways. For instance, gene expression profiles for encoding key enzymes in electron production-transport-consumption process were determine the impact of the alkaline and famine operation on an anammox-centered process (Zhang et al., 2022). For ion or precipitation-mediated anammox process, omics-based evidence is scarce to clarify the discrepant key metabolic pathways (Lin et al., 2019; Xue et al., 2021; Zhen et al., 2021). This knowledge gap requires further investigation to realize the adaptive strategies and regulation mechanism of anammox bacteria. It would provide insights into accelerating anammox cultivation and enhancing the robustness of biological system by identifying the optimal metabolism pathway of anammox consortia.

In this study, we systematically compared ion adsorption and crystal precipitation mediated anammox granulation processes, aiming to answer: (1) which strategy has a better performances by using ion adsorption and crystal precipitation mediated anammox system? (2) how do ion adsorption and crystal precipitation affect anammox granulation? (3) what is the microbial molecular mechanism involved in? With these ideas in mind, the operational performances, anammox activity, sludge characteristics of anammox system mediated by ion adsorption and crystal precipitation were investigated to explore the different anammox granulation process. High-throughput sequencing, metatranscriptomic, and metabolomics approaches were applied to elaborate the underlying mechanism. A strategy for sludge flotation control was proposed. Our study would provide strategies and omics-based evidences for anammox granulation, optimizing the current anammox process.

2. Materials and methods

2.1. Reactor operation

Four Expanded Granular Sludge Bed (EGSB) reactors were conducted to investigate the effects of Mg^{2+} adsorption and MAP crystal (precipitation on anammox granulation process. Reactor 1 (R1) was a control reactor, Reactor 2 (R2) was used to study Mg^{2+} mediated Anammox granulation, and the other two reactors (R3 and R4) were implemented for MAP mediated granulation. The main differences in feeding strategy were shown in Table 1. Substrates and elementary elements were supplied for the basic anammox process in R1. 80 mg L^{-1} of Mg^{2+} was supplied to favor ion adsorption in R2. In R3 and R4, 80 mg L^{-1} of Mg^{2+} coupled with 60 mg L^{-1} of PO_4^{3+}-P were dosed to induce MAP precipitation. Extra crystal seed was added in R4 at the rate of 1.0 g per week, aiming to further promote the crystallization. PO_4^{3+}-P level is used to simulate the swine wastewater (Ye et al., 2016), and Mg/P molar ratio of 1.5~2 is beneficial for the efficient production of MAP (Wang et al., 2018). Mg^{2+} concentration in R2 was kept consistent with R3 and R4 to investigate the sole effect of Mg^{2+} adsorption on anammox process. In phase I (Day 0–56), the set ammonium of R3 and R4 were higher than the nitrite to ensure extra ammonium beyond anammox consumption to form MAP. Afterwards, in phase II (Day 57–207), the influent concentrations of ammonium and nitrite were adjusted to the same level in four reactors for a parallel comparison. See more detailed information given in Text S1.

The EGSB reactor was operated at 33 °C with a working volume of 1.7 L and a hydraulic retention time (HRT) of 9 h (Fig. S1). The seed sludge was obtained from a laboratory anammox reactor under a stable operation for 1.5 years and sieved with 120 mesh sieve. The sludge was parallelly inoculated into four reactors, with the initial mixed liquor suspended solids (MLSS) and mixed liquor volatile suspended solids (MLVSS) of 5.01 and 3.27 g L^{-1}, respectively. A recycle ratio of 16:1 was applied, which corresponded to an upflow velocity of 0.27 mm·s^{-1}. At this flow, the crystal seed would not be washed out from reactors. The height of the expanded sludge bed was 27.0 cm. At the beginning, Ca^{2+} was added as trace element in the influent, so some calcium-like precipitations (HAP, calcium phosphate, etc., Fig. S2-S4 and Text S2) were generated. Subsequently, no extra Ca^{2+} was added in the influent and the relatively pure MAP was generated and coupled with anammox growth in R3 and R4. The date of calcium cutoff was referred to Day 0 in this study. The pH values were maintained at 8.0–8.3 with 1.25 M NaOH to stabilize MAP generation and anammox activity. In addition, PO_4^{3-} was separately pumped from the top of reactors to prevent the influent pipes from precipitation clogging.

2.2. Analysis of water quality and sludge characteristics

A portable pH meter (FG2-FK, METTLER TOLEDO, USA) was used to determine the pH values. The concentrations of NH_4^+-N, NO_2^--N, NO_3^--N, PO_4^{3-}-P and TN in the samples and the MLSS and MLVSS of the sludge were determined according to the standard methods (SEPA, 2002). Inorganic metal ions (Ca^{2+}, Mg^{2+}, Fe^{2+}) were quantified by inductively coupled plasma emission spectrometer (ICP-OES) (ULTIMA 2, HORIBA JY, FR). The specific activities of anammox (SAA) was measured according to the method described in (Wang et al., 2019). The fluoresce heme assay was performed to analyze the heme c content (Sinclair et al., 2001). The wet density of anammox granules were determined according to its movement in sucrose solutions of different densities (Lu et al., 2012), while the granule size was measured by a stereoscopic

Table 1
Different feeding strategy for R1-R4.

Reactor	Mg^{2+} ($mg·L^{-1}$)	PO_4^{3+}-P ($mg·L^{-1}$)	NO_2^--N ($mg·L^{-1}$)	NH_4^+-N ($mg·L^{-1}$)		MAP crystal seed (d = 63–120 μm)
				Phase I	Phase II	
R1	20	6	250	250	380	\
R2	80	6	250	250	380	\
R3	80	60	250	380	380	\
R4	80	60	250	380	380	1.0 g/week

microscope (Nikon, SMZ745T, JPN) coupled with an Image Pro Plus 6.0 software (Lu et al., 2012). The inorganic compositions in sludge were identified by X-ray diffractometer (XRD) (X'Pert Pro, PANalytical B.V., NL). In addition, the granules were further characterized for their morphology and surface element distribution by a Field Emission Scanning Electron Microscopy (FE-SEM) coupled with Energy Dispersive X-Ray Spectroscopy (EDX) (Hitachi S-4800, Hitachi Limited, JPN). All above tests were conducted in triplicates.

2.3. DNA extraction, qPCR, and high-throughput sequencing

The sludge samples were collected from reactors at the end of operation (Day 207). DNA was extracted by the FastDNA® SPIN Kit for Soil (MP Biomedicals, LLC, USA). Quantitative PCR was used to measure the abundance of anammox bacteria (See the primer information and test procedures in Text S3). The V4 variable region of the prokaryotic 16S rRNA gene was amplified using with a unique barcode at the 5-terminal of the consensus forward primer (515F) and reverse primer (806R) (Wang et al., 2019). The collected amplicons were further sequenced on Illumina Miseq sequencing platform (Majorbio, China). The raw data was first filtered and through a quality control using Fastp (version 0.19.6). The processed sequences were then assigned to operational taxonomic units (OTUs) at 97 % similarity level. The OTUs were used for analyzing species annotation of taxonomy in Silva database and community composition. The Circos plot for community composition was drawn using the Circos-0.67–7 software, while the principal component analysis (PCA) and community heatmap were performed in R (version 3.3.1). The sequence data have been deposited into the GenBank sequence read archive (SRA) under Bioproject number PRJNA1130410 and accession numbers SRR29662888-SRR29662899.

2.4. Metatranscriptomic and LC-MS-based metabolomic profiling

The metatranscriptomic and metabolomic analysis were conducted to unravel the mechanisms of Mg^{2+} and MAP-mediated anammox processes. The sludge samples of each reactor were collected in triplicate at the end of the operation for the metatranscriptomic sequencing. The non-rRNA was obtained by removing the ribosomal RNA from the total RNA using Ribo-Zero rRNA Removal Kits (Epicentre, an Illumina® company). Metatranscriptome libraries were sequenced on Illumina Miseq sequencing platform (Majorbio, China). The raw reads were quality filtered by the Seqprep software. rRNA reads were removed using SortMeRNA (v 4.2.0). The open reading frame (ORF) of the obtained transcript sequences was predicted by TransGeneScan, thereby constructing a non-redundant gene set. Then this set was mapped against the KEGG genes database (GENES) using BLASTp (v 2.2.31+) at an E-value cutoff of 1e-5, and annotated by KOBAS 2.0 (KEGG Orthology Based Annotation System). Transcriptional abundances were determined as FPKM (fragments per kilobase of exon model per million mapped reads). The software edgeR was used to compare the transcript levels between samples and identify differentially expressed genes (DEGs) with p value < 0.05 and $|\log_2$ fold change$| > 1$.

Six sludge samples of each reactor were collected at the end of the operation for LC-MS-based non-targeted metabolomic analysis, which was conducted by Majorbio Co., Ltd (Shanghai). The protocols for extracting metabolic products are shown in Text S4. The LC-MS data was uploaded to the Megabio Cloud platform (https://cloud.majorbio.com) for data analysis. The metabolites were annotated against the KEGG database. The differential metabolites were screened with variable importance of projection (VIP) scores >1 and p value < 0.05.

3. Results and discussion

3.1. The effects of Mg^{2+} and MAP on anammox granulation

Exogenous induction of Mg^{2+} and MAP promoted the anammox granulation while differentiated the sludge characteristics. The sludge size in each reactor initially increased rapidly and then gradually declined (Fig. 1(a)). By the end of the operation, all the inoculum sludge developed into granular sludge (> 200 μm) (de Kreuk et al., 2007), with average granule sizes in R3 (263 μm) and R4 (291 μm) being slightly larger than those in R1 (212 μm) and R2 (225 μm) ($p < 0.05$, Fig. S5). Nevertheless, the final sludge densities in R3 and R4 (1.29~1.33 $g{\cdot}cm^{-3}$) were significantly higher than in R1 and R2 (1.04~1.08 $g{\cdot}cm^{-3}$) (Fig. 1(b)).

Mg^{2+} addition enhanced anammox activity while was less effective in increasing sludge density, leading to a considerable sludge loss under the current hydraulic conditions (more information provided below). It halted the continuous size increase of sludge in R2. By contrast, MAP precipitation increased the physical surface area for bacterial colonization and the sludge density as well, and thus benefited anammox sludge retention. Anammox consortia in R3 were more likely to adhere on the surface of newly generated MAP microcrystal rather than the existing MAP-coupled anammox granular sludge. It hindered the sludge in R3 to exhibit a continuous size increase. And, extra periodic dosing of MAP seed in R4 did not further promote sludge growth, because 1) the amount of MAP seeds dosed was low compared to the amount of newly generated MAP, and 2) anammox bacteria were more likely to adhere to the seed rather than the existing MAP-coupled anammox granular sludge, which inhibited the crystal growth of MAP and weaken the effectiveness of the seeding. Overall, both strategies did not significantly increase the particle size of granules. The dosage of Mg^{2+} promoted granulation by stimulating the anammox activity through the potential function of ion adsorption, ion bridging, and electric double layer compression. While MAP generation positively affected the granulation by physically increasing granular density. Other inorganic precipitates, such as zeolite powder and calcium phosphate, were also reported to support granulation in a similar manner (Lin et al., 2020; Liu and Cinquepalmi, 2021).

3.2. Achievement of comparable operating performances by different ways

The reactors were operated for over 200 days to investigate the effects of Mg^{2+} adsorption and MAP precipitation on the long-term nitrogen removal performances in anammox process (Fig. S6). In Phase I (0 day-56 day), nitrogen removal rates (NRR) of R3 and R4 were higher than those of R1 and R2 ($p < 0.01$), with the corresponding maximum values of 1.67–1.70 and 1.24–1.32 kg $N{\cdot}m^{-3}{\cdot}d^{-1}$ (Table S1). It was most likely due to the higher nitrogen loading rate (NLR) in MAP-mediated anammox reactors (R3 and R4) (Tang et al., 2011). To eliminate this variable, the NLRs of four reactors were adjusted to a same level (approximately 1.75 kg $N{\cdot}m^{-3}{\cdot}d^{-1}$) in Phase II (57 day-207 day). During this stage, it can be seen that the NRR and nitrogen removal efficiency (NRE) did not show significant differences among the four reactors ($p > 0.05$). Their average NRR was approximately 1.33 kg $N{\cdot}m^{-3}{\cdot}d^{-1}$, and NRE reached 75 %. Therefore, the presence of Mg^{2+} and MAP did not affect the long-term performances on nitrogen removal.

By further investigating the sludge characteristics, we found both strategies achieved comparable operating performances by using different ways. Mg^{2+} obviously promoted anammox activity, with the highest SAA of 719.6 mg N • g VSS^{-1} • d^{-1} (Fig. 1(c)). Mg^{2+} could act as activators to specifically promote Mg^{2+}-ATPase activities and secretions (Wu et al., 2014) or trigger quorum sensing (Yu et al., 2001; Zhen et al., 2021), which in turn promote energy metabolism and bacterial conversion of substrates. The higher annamox activity in R2 was also related to more abundant heme c content in the sludge (Fig. 1(d)). Heme c is an essential catalytic cofactor for nitrite reductase (Nir), hydrazine synthase (HZS), and hydroxylamine oxidoreductase (HAO) involved in anammox process, and acts as protein derivative participating in electron transfer and storage (Kartal and Keltjens, 2016; Ma et al., 2019). Accordingly, heme c and SAA had a positive relationship (Chen et al.,

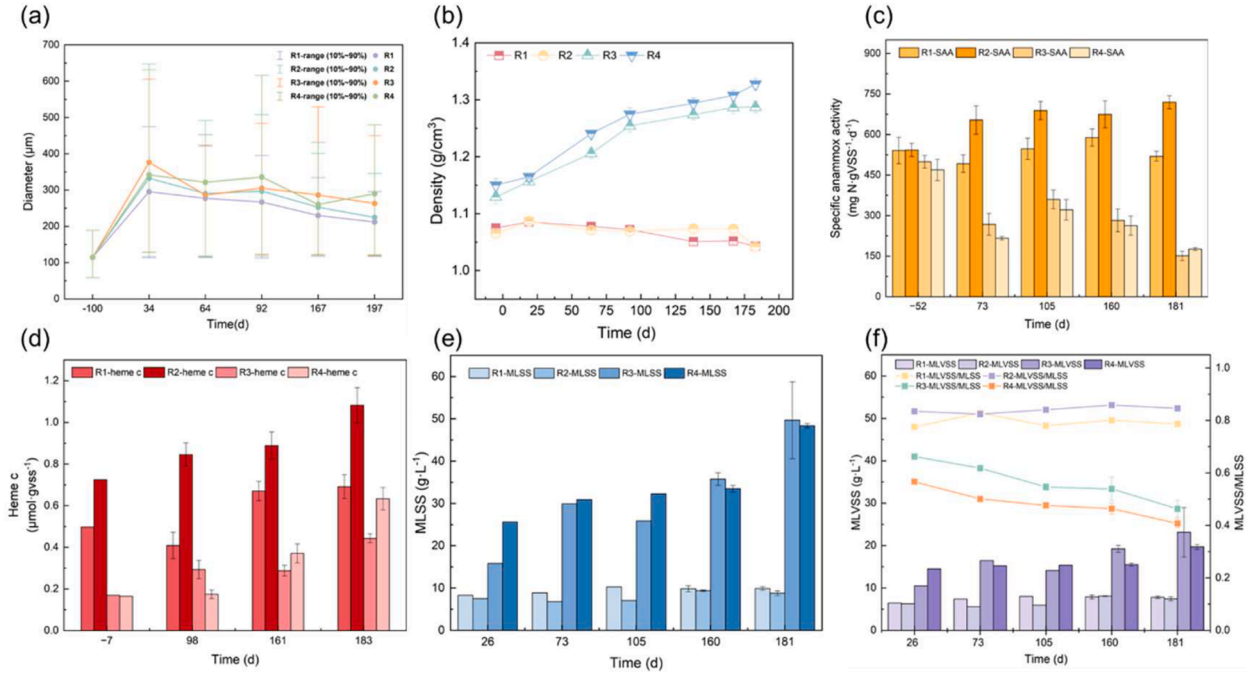

Fig. 1. Variations in sludge characteristics over time. (a) particle size; (b) sludge density; (c) SAA; (d) heme c content; (e) MLSS; (f) MLVSS and the ratio of MLVSS and MLSS.

2013; Jin et al., 2013). However, the MLSS and MLVSS in R2 were comparable or even lower than the control, most likely due to the sludge loss, causing by the high SAA.

On the other hand, the MAP precipitation negatively affected the annamox activity. The SAA of MAP precipitation-mediated reactors (R3 and R4) decreased to 151.5~176.2 mg N·gVSS^{-1}·d^{-1} from 469.3~499.2 mg N·gVSS^{-1}·d^{-1}, even lower than that in the control reactor (519.6 mg N·gVSS^{-1}·d^{-1}) (Fig. 1(c)). Whilst, the MAP production significantly increased the growth rate of anammox sludge. After operation for 181 days, compared to the control reactor, the MLSS in R3 and R4 increased by 400.8 % and 387.6 %, respectively, while the MLVSS in there were improved by 196.9 % and 152.7 %, respectively (Fig. 1(e)(f)).

We calculated the overall nitrogen removal capacities (SAA×MLVSS), which were 4052.9, 5354.0, 3508.7, and 3374.4 mg N·L^{-1}·d^{-1} for R1-R4, respectively. By the end of the operation, MAP production did not significantly influence the overall operating performances, as reflected in the effluent quality mentioned above. Therefore, both strategies came to comparable nitrogen removal performances: Mg^{2+} addition was associated with high SAA and low biomass, while MAP generation resulted in low SAA and high biomass. It should be noted that excessive precipitation growth in the granules may harm the anammox process due to an inadequate substrate mixture in a high-density sludge granular (Polizzi et al., 2022; Trigo et al., 2006), and we are still working on the threshold.

3.3. *Generation of MAP in anammox granular sludge enhances flotation control*

Both Mg^{2+} and PO_4^{3-} were rarely removed at pH of 7.6–8.0 in R3 and R4, indicating that no MAP was generated. However, their co-removal was observed there from Day 56 when pH increased to 8.0–8.2 (Fig. S7). By contrast, there was almost no consumption of Mg^{2+} and PO_4^{3-} in R1 and R2 (Fig. S8). The removal molar ratio of Mg^{2+} and PO_4^{3-}-P in R3 (1:0.88) and R4 (1:0.97) was close to the stoichiometric ratio (1:1) for MAP formation. This phenomenon indicated the MAP generation during autotrophic nitrogen removal process, which was verified by XRD. It was shown that the relatively pure MAP crystals were formed without other crystal species identified (Fig. 2(a)). The images of stereoscopic microscope and SEM also indicated the presence of MAP in annamox granular, where the prismy and orthorhombic precipitates represented the typical structures of MAP (Ye et al., 2014) (Fig. 2 (b)-(e)). These precipitates could serve as the combining sites for microbial aggregation (Guo et al., 2021).

MAP generation led to differences in micromorphology, color, and sludge yield among reactors. Specifically, the elliptical bacteria with volcanic crater-like concaves assembled and tightly integrated with each other in R1 and R2, whereas the precipitates were embedded in anammox biomass in R3 and R4 (Fig. S9). The color of anammox sludge was reddish in R1, scarlet in R2, but red alternating with white in R3 and R4. The ratios of MLVSS and MLSS in R3 (0.46) and R4 (0.41) were lower than that in R1 (0.79) and R2 (0.85) (Fig. 1(f)), due to a faster accumulation of MAP than biomass.

MAP generation also increased the density of granular sludge, and hence effectively improved the sludge sedimentation performance. We withdrew 250 mL of the mixed activated sludge from each reactor and settled the mixture for 30 min. A severe sludge flotation was observed in R2, followed by R1, while almost no sludge floatation happened for R3 and R4 (Fig. S10). This enhancement effect on sedimentation was also reported for calcium-like precipitates, such as HAP, which acted as skeletons to prevent anammox particles bulking and floating (Ma et al., 2018; Xue et al., 2021). During the operation, sludge floatation periodically appeared on Day 74–83 and Day 138–162 in R1, and on Day 69–73 and Day 145–200 in R2. The daily loss amounts of sludge were at 0.11, 0.17, 0.01, and 0.04 g SS d^{-1} for R1, R2, R3, and R4, respectively. The large amount of washed out sludge in R2 caused a sharp decrease in its height of sludge bed expansion (Fig. S11). It was most likely due to high NRR and SAA in R2. Thus, we conclude that Mg^{2+}-mediated biological process significantly enhances anammox activity, yet a number of produced N_2-bubbles results in a severe sludge flotation. On the contrary, MAP-coupled anammox granular sludge with high density can be effectively retained in reactors. Therefore, the sludge flotation can be controlled by developing precipitates-coupled anammox sludge.

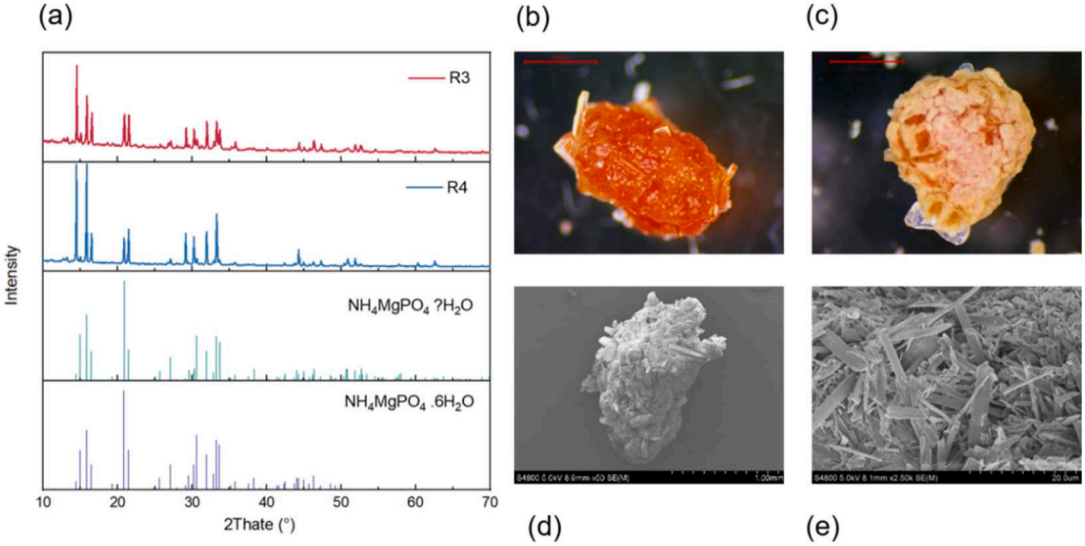

Fig. 2. Co-growth of MAP and biomass in R3 and R4. (a) XRD results; (b, c) the images of stereoscopic microscope; (d, e) FE-SEM.

3.4. Changes in community structure and gene quantification

The microbial community composition of each reactor at the phylum level was shown in Fig. 3(a). There was no significant differences among the four reactors. *Planctomycetes*, to which most anammox bacteria belonging, was absolutely dominant. Other bacteria were assigned to *Bacteroidota, Proteobacteria*, and *Chloroflexi*, which also commonly appeared in the anammox system (Chen et al., 2016; Chu et al., 2015; Connan et al., 2016). They are involved in activities such as consuming decaying anammox bacterial cells, carrying out partial denitrification to provide nitrite for anammox, and providing secondary metabolites in cross-feeding (Kindaichi et al., 2012; Lawson et al., 2017; Zhao et al., 2018b). Most N-cycling microorganism acting as denitrifiers belonged to *Proteobacteria* (Lawson et al., 2017). Both *Chloroflexi* and *Bacteroidetes* were associated with the formation of granular sludge. The former may form the initial framework for sludge particles, and the later preferred to attach to the outer layer of sludge particles, building a meshwork structure for adherence (Cao et al., 2016). It is widely recognized that anammox granules facilitate multiple reactions, in which a diverse, multitrophic, cooperative/competitive microbial community is established and plays a crucial role in supporting nitrogen removal processes.

The heatmap visualization of hierarchical clustering at the genus

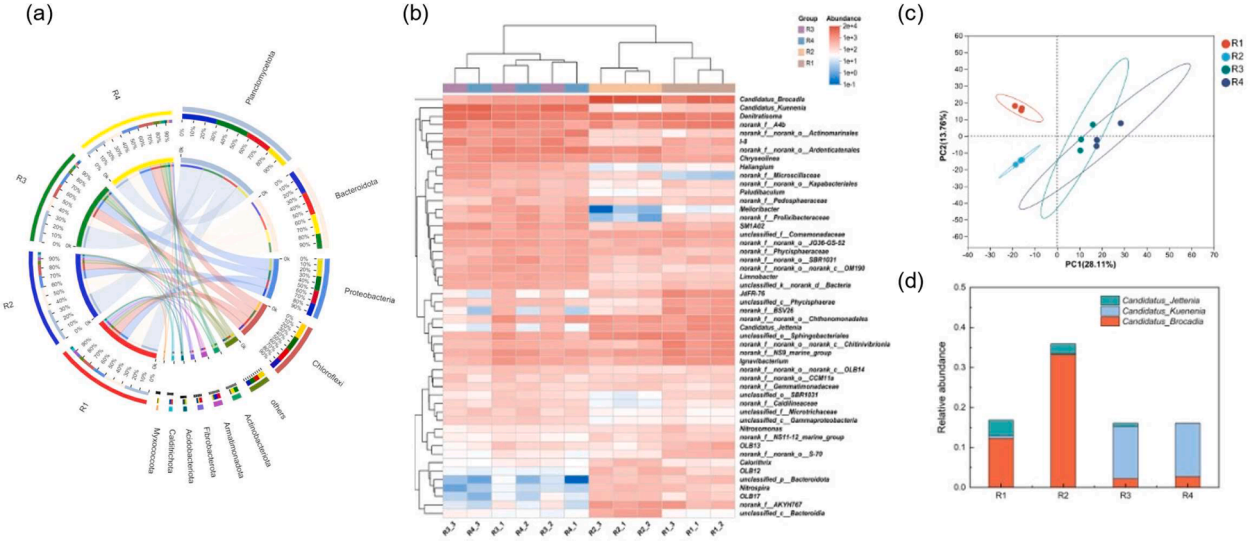

Fig. 3. Microbial community composition in different reactors. (a) Community composition at phylum levels. The left half circle indicates the species composition in different reactors, the color of the outer colored band represents the different reactors, the color of the inner colored band represents the species, and the length represents the relative abundance of species in the corresponding reactor; the right half circle indicates the proportion of species distribution in different reactors, the outer colored band represents the species, the color of the inner colored band represents different reactors, and the length represents the proportion of distribution of the reactor in a particular species. (b) Hierarchical clustering of the top 50 ranked genus-level community members of four reactors. (c) PCA analysis at genus level. (d) The abundances of the identified anammox bacteria in four reactors.As a whole, the relative abundance of anammox bacteria were 16.83 %, 35.93 %, 16.07 %, and 16.07 % for R1-R4, respectively. We also quantified the absolute abundance of anammox bacteria on Day 65, 99, 139, and 177 for R1-R4 using qPCR (Fig. S12 (a)). Both results confirmed that anammox bacteria proliferated massively in R2, suggesting that the appropriate addition of Mg^{2+} may support anammox proliferation. Moreover, anammox abundance increased with the granule size, as such, the particle with a size of >500 μm contained the highest copy number of anammox 16 s rDNA gene (Fig. S12(b)). The sequencing and qPCR results presented here could support the aforementioned experimental data and further demonstrated the different effects of two strategies on anammox granulation processes.

level (Fig. 3(b)) showed that *Ca. Brocadia, Ca. Kuenenia*, and *Denitratisoma* were the most enriched bacteria. *Ca. Brocadia* and *Ca. Kuenenia* were ubiquitous anammox bacteria (Tang et al., 2017). *Denitratisoma* was a denitrifying bacteria, which could synergistically remove nitrogen with anammox bacteria for a high nitrogen removal efficiency (Wang et al., 2023a). All the top 3 genus involved in biological nitrogen conversion. Other species also contributed to the efficient functioning of anammox system. For example, *SM1A02* was identified to have the capacity of autotrophic nitrogen removal (Yang et al., 2023). *Chryseolinea* promoted the secretion of polysaccharide in EPS to aid the granules formation (Grasso et al., 2002; Miao et al., 2018).

PCA analysis at genus level showed that R3 and R4 overlapped with each other, but were clearly separated from R1 and R2 (Fig. 3(c)). It indicated that either Mg^{2+} addition or MAP generation significantly affected the microbial community succession. We calculated the relative abundance of three typical anammox bacteria including *Ca. Brocadia, Ca. Kuenenia*, and *Ca. Jettenia*, and exhibited their distribution in each reactor (Fig. 3(d)). *Ca. Brocadia* was most responsible for anammox capacity in R1 and R2, while the key functional bacteria shifted to *Ca. Kuenenia* in R3 and R4. In addition, *Ca. Jettenia* accounted for a small amount in R1 and R2, which can be explained by the fact that *Ca. Jettenia* often exists in small-size particles (< 200 μm) (Liu et al., 2017). *Ca. Brocadia* was reported to have a higher anammox activity compared to *Ca. Kuenenia* (Oshiki et al., 2016), which may contribute to the higher SAA in R1 and R2 (Fig. 1(c)). On the other hand, the mineral composition in the sludge from R3 and R4 might promote *Ca. Kuenenia* to outcompete *Ca. Brocadia*, as also previously observed by Pollizzi (2022). This was because that *Ca. Brocadia* preferred the substrate-rich environments, but *Ca. Kuenenia* has a higher substrate affinity (Oshiki et al., 2016; van der Star et al., 2008). Moreover, the higher pH in R3 and R4 may also assist *Ca. Kuenenia* with this competition as it is more alkaline tolerant than *Ca. Brocadia* (Egli et al., 2001). Therefore, *Ca. Kuenenia* could more tolerate the conditions of mass transfer limitation and alkaline, then gradually became dominant in R3 and R4.

3.5. Discrepancies in metatranscriptomic and metabolic outputs for anammox granulation and activity

For Mg^{2+}-mediated anammox process, we found that the differential metabolites within the glycerophospholipid metabolic pathway were enriched in R2, which is a relatively intact biosynthesis pathways of Phosphatidylethanolamine (PtE) (Zhao et al., 2018a). However, these metabolites were noticed to be diminished in R3 and R4 (Fig. 4). The enhanced PtE biosynthesis in R2 intensified extracelluar phospholipid secretion, contributing to the biomass aggregation. By contrast, anammox granulation in R3 and R4 predominantly reflected in the sludge density rather than particle size, which was induced by the co-growth of anammox bacteria with high-density MAP. It is a physical process, and thus we could not obtain enough microbial evidence to support it.

Meanwhile, anammox activity was affected by these two strategies, which could be explained in terms of energy metabolism. For nitrogen metabolism, the oxidation of N_2H_4 is a key electron generation process via nitrogen metabolism. These electrons are indirectly transferred to nitrite reductase (NIR) and hydrazine synthase (HZS) via quinone pool and cyt bc 1(Strous et al., 2006), coupling with NADH generation (Kouba et al., 2022). It can be observed that the mRNA expressions of hzs were upregulated by 2.17-, 11.03-, and 17.99-fold in R2, R3, and R4 compared to R1. Under environmental stress, anammox bacteria attempted to up-regulate gene expression levels for energy harvest (Ma et al., 2020; Zhao et al., 2018a). These regulations for nitrogen conversion metabolism indicated the increases in anammox activities and growth (Bagchi et al., 2016). On the other hand, the oxidation of nitrite to nitrate by nitrite oxidoreductase (NXR) can replenish the electrons consumed by anammox for carbon fixation (Kartal and Keltjens, 2016). In autotrophic anammox bacteria, Wood-Ljungdahl pathway (WLP) is responsible for the CO_2 utilization and acetyl-CoA generation, which further produces NADH through the tricarboxylic acid (TCA) cycle (Zhang et al., 2022). Inorganic carbon metabolism was barely changed in Mg^{2+}-mediated anammox process (R2), but was down-regulated in MAP-mediated process (R3 and R4) (Fig. 4). In contrast, some metabolites involved in WLP was enriched in R2, but still maintained in

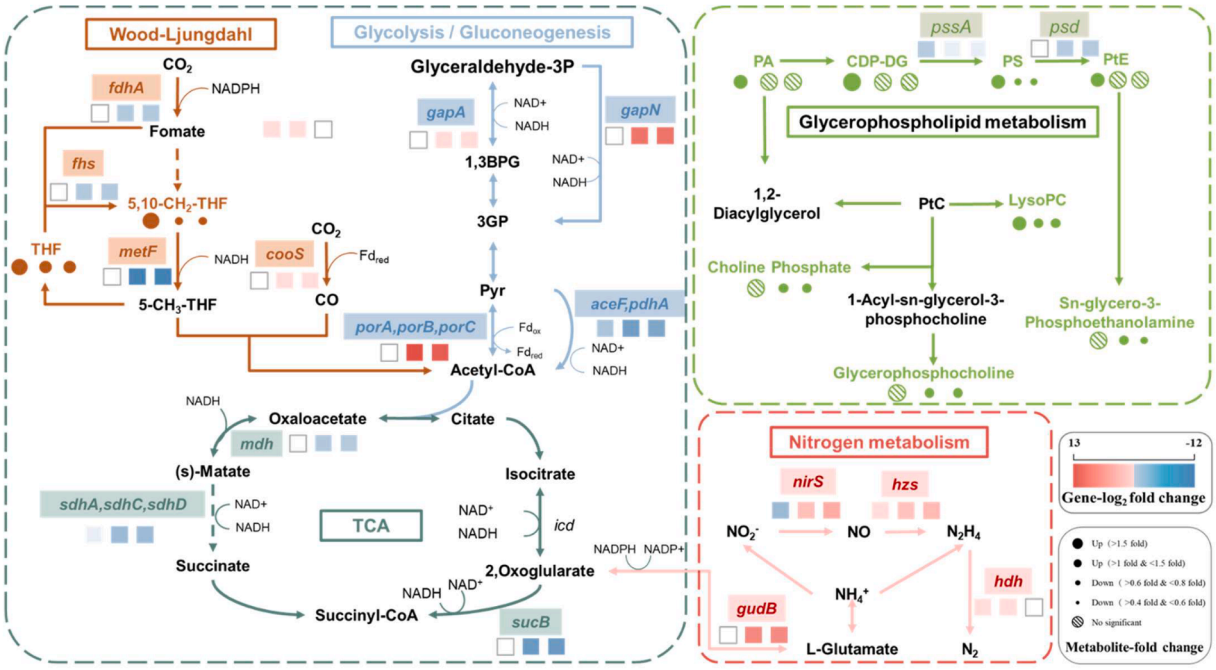

Fig. 4. Central differential gene expression and differential metabolites of the predominant *Ca. Kuenenia & Ca. Brocadia*. The arrows of different colors represent reactions of nitrogen metabolism, WLP, gluconeogenesis, TCA cycle, and Glycerophospholipid metabolism respectively; the boxes of the corresponding colors are the differentially expressed genes in each metabolic pathway; the three squares and dots below represent the gene changes and metabolites of R2, R3, R4 versus R1 from left to right, respectively. The colors of squares represent up-down regulated genes and sizes of dots represent up-down regulated metabolites.

relatively low levels in R3 and R4 (Fig. 4). In addition, anammox bacteria are capable of metabolizing organic carbon (Ji et al., 2021), which was scarcely expressed in R2 but strengthened in R3 and R4 (Fig. 4). All these variations in the electron flow led to an efficient nitrogen removal. Specifically, synchronous upregulation in both nitrogen and inorganic carbon metabolisms for energy generation may be responsible for high anammox activity in R2. However, it was speculated that extra precipitates formed in R3 and R4 caused mass transfer limitation and hence downregulated the inorganic carbon metabolism. As a response, the gene upregulations of nitrogen metabolism and organic carbon metabolism (glycolysis/gluconeogenesis) could counteract the disadvantages and alleviate energy limitation. Similarly, *Ca. Brocadia fulgida* was reportedly adopted this strategy to adapt to cold stress (Huo et al., 2020). Interestingly, when the feeding $NaHCO_3$ concentration increased from 1048 mg L^{-1} to 1500 mg L^{-1}, both downregulation of inorganic carbon metabolism pathway and upregulation of organic carbon metabolism pathway were attenuated in R3 and R4. (Fig. S13). This indeed confirmed our hypothesis that the precipitates inhibited the mass transfer and therefore reduced the anammox activity.

3.6. Implication for field applications

The above observations indicate that co-growth of crystal precipitation and anammox bacteria is beneficial for granule formation and flotation control. In the field, the type of crystal precipitation could be chosen depending on the mineral composition of intake wastewater. For instance, MAP crystal is a promising option for the Mg^{2+} and P enriched wastewater, whereas hydroxyapatite can be an alternative when the intake water contains abundant Ca^{2+} and P (Xue et al., 2021). A mixture of multiple crystal precipitates may work to the wastewater containing a complex mineral matrix. By analogy, carbon-based, iron-based, silicon-based materials etc. could be dosed as cores to accelerate formation of anammox granules (Wang et al., 2023b). It is worthwhile to further investigate how these different crystals affect the annamox granulation and activity so that we can provide both technically and economically wise recommendations for practical application under variable conditions. Although the robustness of operational performances in anammox system employing this strategy is still being worked on, these approaches could potentially be adapted for other granular sludge systems.

4. Conclusion

Mg^{2+}- and MAP-mediated anammox granulation processes exhibited different sludge characteristics and regulation mechanisms. The presence of Mg^{2+} (80 mg L^{-1} in our study) activated nitrogen and inorganic carbon metabolisms, increased heme c concentration to strengthen electron transfer, thereby boosting anammox activity. Although more EPS was secreted for self-aggregation and granulation, a large amount of produced N_2-bubbles was encapsulated inside or adhered to particle surfaces, reducing sludge density and ultimately causing sludge floatation. In contrast, MAP-mediated anammox granulation reduced heme c content and anammox activity due to the inhibition of inorganic carbon fixation. As a compensatory response, nitrogen and organic carbon metabolisms were up-regulated to alleviate energy crisis. MAP precipitates provided a physical structure for microbial interaction, supporting to form granules with a high density. Despite the decrease in SAA, a comparable nitrogen removal performance was achieved due to more retention of biomass. Co-growth of MAP and anammox sludge may represent a promising approach to efficiently control sludge flotation. Our study provides transcriptomic and metabolomic insights into anammox granulation and operation mediated by exogenous induction of ion and precipitation, which advances the current understanding of anammox process.

CRediT authorship contribution statement

Huiqun Shi: Writing – original draft, Visualization, Investigation, Formal analysis, Data curation. **Xiaoyi Ren:** Visualization, Validation, Investigation, Formal analysis, Data curation. **Ruili Yang:** Methodology, Funding acquisition, Formal analysis. **Jinsong Wang:** Writing – review & editing. **Huaihao Xu:** Formal analysis, Writing – review & editing. **Xinqing Liao:** Project administration, Methodology. **Yaoyin Lou:** Methodology. **Shaohua Chen:** Supervision, Resources, Funding acquisition. **Xin Ye:** Writing – review & editing, Supervision, Funding acquisition. **Xiaojun Wang:** Writing – review & editing, Supervision, Resources, Methodology, Funding acquisition, Conceptualization.

Declaration of competing interest

The authors declare that they have no known competing financial interests or personal relationships that could have appeared to influence the work reported in this paper.

Acknowledgements

This research was financially supported by the Science and Technology Program of Fujian Province (2023Y0073), the National Natural Science Foundation of China (51708536), the Funding for School-level Research Projects of Yancheng Institute of Technology (xjr2022032), and the Natural Science Foundation of the Jiangsu Higher Education Institutions of China (23KJD610004).

Supplementary materials

Supplementary material associated with this article can be found, in the online version, at doi:10.1016/j.watres.2024.122954.

Data availability

Data will be made available on request.

References

Bagchi, S., Lamendella, R., Strutt, S., Van Loosdrecht, M.C.M., Saikaly, P.E., 2016. Metatranscriptomics reveals the molecular mechanism of large granule formation in granular anammox reactor. Sci. Rep. 6.
Cao, S.B., Du, R., Li, B.K., Ren, N.Q., Peng, Y.Z., 2016. High-throughput profiling of microbial community structures in an ANAMMOX-UASB reactor treating high-strength wastewater. Appl. Microbiol. Biotechnol. 100 (14), 6457–6467.
Chen, C.J., Sun, F.Q., Zhang, H.Q., Wang, J.F., Shen, Y.L., Liang, X.Q., 2016. Evaluation of COD effect on anammox process and microbial communities in the anaerobic baffled reactor (ABR). Bioresour. Technol. 216, 571–578.
Chen, J.W., Ji, Q.X., Zheng, P., Chen, T.T., Wang, C.H., Mahmood, Q., 2010. Floatation and control of granular sludge in a high-rate anammox reactor. Water Res. 44 (11), 3321–3328.
Chen, T.T., Zheng, P., Shen, L.D., 2013. Growth and metabolism characteristics of anaerobic ammonium-oxidizing bacteria aggregates. Appl. Microbiol. Biotechnol. 97 (12), 5575–5583.
Chu, Z.R., Wang, K., Li, X.K., Zhu, M.T., Yang, L., Zhang, J., 2015. Microbial characterization of aggregates within a one-stage nitritation-anammox system using high-throughput amplicon sequencing. Chem. Eng. J. 262, 41–48.
Connan, R., Dabert, P., Khalil, H., Bridoux, G., Beline, F., Magri, A., 2016. Batch enrichment of anammox bacteria and study of the underlying microbial community dynamics. Chem. Eng. J. 297, 217–228.
de Kreuk, M.K., Kishida, N., van Loosdrecht, M.C.M., 2007. Aerobic granular sludge - state of the art. Water Sci. Technol. 55 (8–9), 75–81.
Egli, K., Fanger, U., Alvarez, P.J.J., Siegrist, H., van der Meer, J.R., Zehnder, A.J.B., 2001. Enrichment and characterization of an anammox bacterium from a rotating biological contactor treating ammonium-rich leachate. Arch. Microbiol. 175 (3), 198–207.
Fu, J.X., Zhou, M.J., Yun, J., Su, Y., Yu, P.F., Sun, M., Ji, X.Q., 2017. The effect of divalent metal ions and recycle ratio of uasb reactor on the formation of anammox granules and its treatment performance. Water, Air, & Soil Pollution 228 (11), 411.
Grasso, D., Subramaniam, K., Butkus, M., Strevett, K., Bergendahl, J., 2002. A review of non-DLVO interactions in environmental colloidal systems. Rev. Environ. Sci. Biotechnol. 1 (1), 17–38.
Guo, Y., Xie, C.L., Chen, Y.J., Urasaki, K., Qin, Y., Kubota, K., Li, Y.Y., 2021. Achieving superior nitrogen removal performance in low-strength ammonium wastewater

treatment by cultivating concentrated, highly dispersive, and easily settleable granule sludge in a one-stage partial nitritation/anammox-HAP reactor. Water Res. 200.
Huo, T.R., Zhao, Y.P., Tang, X., Zhao, H.Z., Ni, S.Q., Gao, Q., Liu, S.T., 2020. Metabolic acclimation of anammox consortia to decreased temperature. Environ. Int. 143.
Ji, X.M., Zheng, C., Wang, Y.L., Jin, R.C., 2021. Decoding the interspecies interaction in anammox process with inorganic feeding through metagenomic and metatranscriptomic analysis. J. Clean. Prod. 288.
Jiang, H.L., Tay, J.H., Liu, Y., Tay, S.T.L., 2003. Ca^{2+} augmentation for enhancement of aerobically grown microbial granules in sludge blanket reactors. Biotechnol. Lett. 25 (2), 95–99.
Jin, R.C., Zhang, Q.Q., Yang, G.F., Xing, B.S., Ji, Y.X., Chen, H., 2013. Evaluating the recovery performance of the ANAMMOX process following inhibition by phenol and sulfide. Bioresour. Technol. 142, 162–170.
Kartal, B., Keltjens, J.T., 2016. Anammox Biochemistry: a Tale of Heme *c* Proteins. Trends Biochem. Sci. 41 (12), 998–1011.
Kartal, B., Kuenen, J.G., van Loosdrecht, M.C.M., 2010. Sewage Treatment with Anammox. Science (1979) 328 (5979), 702–703.
Kindaichi, T., Yuri, S., Ozaki, N., Ohashi, A., 2012. Ecophysiological role and function of uncultured Chloroflexi in an anammox reactor. Water Sci. Technol. 66 (12), 2556–2561.
Kouba, V., Bachmannova, C., Podzimek, T., Lipovova, P., van Loosdrecht, M.C.M., 2022. Physiology of anammox adaptation to low temperatures and promising biomarkers: a review. Bioresour. Technol. 349.
Lawson, C.E., Wu, S., Bhattacharjee, A.S., Hamilton, J.J., McMahon, K.D., Goel, R., Noguera, D.R., 2017. Metabolic network analysis reveals microbial community interactions in anammox granules. Nat. Commun. 8.
Li, J.Y., Chen, Z.G., Zhang, Y.Z., Zhang, Y., Yang, J.F., Li, B.Q., Tang, X., Li, K.M., Wang, X.J., 2024. Simultaneous nitrogen removal and phosphorus recovery by anammox-induced magnesium phosphate mineralization: interaction mechanism between microorganisms and mineral formation. ACS Sustain. Chem. Eng. 12 (19), 7392–7401.
Lin, H.H., Ma, R., Lin, J.H., Sun, S.C., Liu, X.L., Zhang, P.X., 2020. Positive effects of zeolite powder on aerobic granulation: nitrogen and phosphorus removal and insights into the interaction mechanisms. Environ. Res. 191.
Lin, L., Zhang, Y.L., Beckman, M., Cao, W.Z., Ouyang, T., Wang, S.P., Li, Y.Y., 2019. Process optimization of anammox-driven hydroxyapatite crystallization for simultaneous nitrogen removal and phosphorus recovery. Bioresour. Technol. 290.
Liu, W.R., Yang, D.H., Chen, W.J., Gu, X., 2017. High-throughput sequencing-based microbial characterization of size fractionated biomass in an anoxic anammox reactor for low-strength wastewater at low temperatures. Bioresour. Technol. 231, 45–52.
Liu, Y., Yang, S.F., Tay, J.H., Liu, Q.S., Qin, L., Li, Y., 2004. Cell hydrophobicity is a triggering force of biogranulation. Enzyme Microb. Technol. 34 (5), 371–379.
Liu, Y.Q., Cinquepalmi, S., 2021. Exploration of mechanisms for calcium phosphate precipitation and accumulation in nitrifying granules by investigating the size effects of granules. Water Res. 206.
Lu, H.F., Zheng, P., Ji, Q.X., Zhang, H.T., Ji, J.Y., Wang, L., Ding, S., Chen, T.T., Zhang, J. Q., Tang, C.J., Chen, J.W., 2012. The structure, density and settlability of anammox granular sludge in high-rate reactors. Bioresour. Technol. 123, 312–317.
Ma, H.Y., Zhang, Y., Xue, Y., Li, Y.Y., 2018. A new process for simultaneous nitrogen removal and phosphorus recovery using an anammox expanded bed reactor. Bioresour. Technol. 267, 201–208.
Ma, H.Y., Zhang, Y.L., Xue, Y., Zhang, Y.F., Li, Y.Y., 2019. Relationship of heme c, nitrogen loading capacity and temperature in anammox reactor. Sci. Total Environ. 659, 568–577.
Ma, X., Yan, Y., Wang, W.G., Guo, J.H., Wang, Y.Y., 2020. Metatranscriptomic analysis of adaptive response of anammox bacteria *Candidatus* 'Kuenenia stuttgartiensis' to Zn (II) exposure. Chemosphere 246.
Miao, L., Zhang, Q., Wang, S.Y., Li, B.K., Wang, Z., Zhang, S.J., Zhang, M., Peng, Y.Z., 2018. Characterization of EPS compositions and microbial community in an Anammox SBBR system treating landfill leachate. Bioresour. Technol. 249, 108–116.
Oshiki, M., Satoh, H., Okabe, S., 2016. Ecology and physiology of anaerobic ammonium oxidizing bacteria. Environ. Microbiol. 18 (9), 2784–2796.
Pol, L.W.H., Lopes, S.I.D., Lettinga, G., Lens, P.N.L., 2004. Anaerobic sludge granulation. Water Res. 38 (6), 1376–1389.
Polizzi, C., Lotti, T., Ricoveri, A., Campo, R., Vannini, C., Ramazzotti, M., Gabriel, D., Munz, G., 2022. Long-term effects of mineral precipitation on process performance, granules' morphology and microbial community in anammox granular sludge. J. Environ. Chem. Eng. 10 (1).
SEPA, 2002. Monitoring and Analytical Methods of Water and Wastewater. China Environmental Science Press, Beijing.
Sinclair, P.R., Gorman, N., Jacobs, J.M., 2001. Measurement of heme concentration. Curr. Protoc. Toxicol. Chapter 8. Unit 8.3-Unit 8.3.
Song, Y.X., Liao, Q., Yu, C., Xiao, R.Y., Tang, C.J., Chai, L.Y., Duan, C.S., 2017. Physicochemical and microbial properties of settled and floating anammox granules in upflow reactor. Biochem. Eng. J. 123, 75–85.
Strous, M., Pelletier, E., Mangenot, S., Rattei, T., Lehner, A., Taylor, M.W., Horn, M., Daims, H., Bartol-Mavel, D., Wincker, P., Barbe, V., Fonknechten, N., Vallenet, D., Segurens, B., Schenowitz-Truong, C., Médigue, C., Collingro, A., Snel, B., Dutilh, B. E., Op den Camp, H.J.M., van der Drift, C., Cirpus, I., van de Pas-Schoonen, K.T., Harhangi, H.R., van Niftrik, L., Schmid, M., Keltjens, J., van de Vossenberg, J., Kartal, B., Meier, H., Frishman, D., Huynen, M.A., Mewes, H.W., Weissenbach, J., Jetten, M.S.M., Wagner, M., Le Paslier, D., 2006. Deciphering the evolution and metabolism of an anammox bacterium from a community genome. Nature 440 (7085), 790–794.
Tang, C.J., Duan, C.S., Yu, C., Song, Y.X., Chai, L.Y., Xiao, R.Y., Wei, Z.S., Min, X.B., 2017. Removal of nitrogen from wastewaters by anaerobic ammonium oxidation (ANAMMOX) using granules in upflow reactors. Environ. Chem. Lett. 15 (2), 311–328.
Tang, C.J., Zheng, P., Wang, C.H., Mahmood, Q., Zhang, J.Q., Chen, X.G., Zhang, L., Chen, J.W., 2011. Performance of high-loaded ANAMMOX UASB reactors containing granular sludge. Water Res. 45 (1), 135–144.
Trigo, C., Campos, J.L., Garrido, J.M., Mendez, R., 2006. Start-up of the Anammox process in a membrane bioreactor. J. Biotechnol. 126 (4), 475–487.
van der Star, W.R.L., Miclea, A.I., van Dongen, U.G.J.M., Muyzer, G., Picioreanu, C., van Loosdrecht, M.C.M., 2008. The membrane bioreactor: a novel tool to grow anammox bacteria as free cells. Biotechnol. Bioeng. 101 (2), 286–294.
Wang, D.P., Luo, Q., Huang, K.L., Zhang, X.X., 2023a. Distinct mechanisms underlying assembly processes and interactions of microbial communities in two single-stage bioreactors coupling anammox with denitrification. Chem. Eng. J. 452.
Wang, J.S., Ye, X., Zhang, Z.J., Ye, Z.L., Chen, S.H., 2018. Selection of cost-effective magnesium sources for fluidized struvite crystallization. J. Environ. Sci. 70, 144–153.
Wang, P.C., Lu, B., Liu, X.J., Chai, X.L., 2023b. Accelerating the granulation of anammox sludge in wastewater treatment with the drive of "micro-nuclei": a review. Sci. Total Environ. 860.
Wang, X.J., Yang, R.L., Guo, Y., Zhang, Z.L., Kao, C.M., Chen, S.H., 2019. Investigation of COD and COD/N ratio for the dominance of anammox pathway for nitrogen removal via isotope labelling technique and the relevant bacteria. J. Hazard. Mater. 366, 606–614.
Wu, P., Wang, Y.L., Zhang, G.M., Liu, X.S., Du, C., Tong, Q.Y., Li, N., 2014. Improving biomass resource recycling capacity of Rubrivivax gelatinosus cultivated in wastewater through regulating the generation and use of energy. Environ. Technol. 35 (20), 2604–2609.
Wu, P., Zhang, G.M., Li, J.Z., 2015. Mg^{2+} improves biomass production from soybean wastewater using purple non-sulfur bacteria. J. Environ. Sci. 28, 43–46.
Xue, Y., Ma, H.Y., Kong, Z., Li, Y.Y., 2021. Formation Mechanism of hydroxyapatite encapsulation in Anammox-HAP Coupled Granular Sludge. Water Res. 193.
Yang, R.L., Li, Y.A., Chen, J.L., Wu, J.B., Zhang, S.C., Chen, S.H., Wang, X.J., 2023. Characteristics variations of size-fractionated anammox granules and identification of the potential effects on these evolutions. Environ. Res. 237.
Ye, X., Ye, Z.-L., Lou, Y.Y., Pan, S.Q., Wang, X., Wang, M.K., Chen, S.H., 2016. A comprehensive understanding of saturation index and upflow velocity in a pilot-scale fluidized bed reactor for struvite recovery from swine wastewater. Powder Technol. 295, 16–26.
Ye, Z.L., Shen, Y., Ye, X., Zhang, Z.J., Chen, S.H., Shi, J.W., 2014. Phosphorus recovery from wastewater by struvite crystallization: property of aggregates. J. Environ. Sci. 26 (5), 991–1000.
Yu, H.Q., Tay, J.H., Fang, H.H.P., 2001. The roles of calcium in sludge granulation during UASB reactor start-up. Water Res. 35 (4), 1052–1060.
Zhang, L., Hao, S.W., Dou, Q.H., Dong, T.J., Qi, W.K., Huang, X.W., Peng, Y.Z., Yang, J. C., 2022. Multi-omics analysis reveals the nitrogen removal mechanism induced by electron flow during the start-up of the anammox- centered process. Environ. Sci. Technol. 56, 16115–16124.
Zhang, Z.Z., Xu, J.J., Hu, H.Y., Shi, Z.J., Ji, Z.Q., Deng, R., Shi, M.L., Jin, R.C., 2016. Insight into the short- and long-term effects of inorganic phosphate on anammox granule property. Bioresour. Technol. 208, 161–169.
Zhao, Y.P., Feng, Y., Li, J.Q., Guo, Y.Z., Chen, L.M., Liu, S.T., 2018a. Insight into the aggregation capacity of anammox consortia during reactor start-up. Environ. Sci. Technol. 52 (6), 3685–3695.
Zhao, Y.P., Liu, S.F., Jiang, B., Feng, Y., Zhu, T.T., Tao, H.C., Tang, X., Liu, S.T., 2018b. Genome-centered metagenomics analysis reveals the symbiotic organisms possessing ability to cross-feed with anammox bacteria in anammox consortia. Environ. Sci. Technol. 52 (19), 11285–11296.
Zhen, J.Y., Cui, Q.J., Liu, X.L., Yu, Z.B., Wang, C.F., Ni, S.Q., 2021. Unravelling the importance of Ca^{2+} and Mg^{2+} as essential in anammox culture medium. Bioresour. Technol. 340, 125729.